Final Report relative to AWARD No. FA8655-03-1-3017 by

dr. Rita Magri

(Period of performance Nov. 2002 – Nov.2004)

1) Calculation of the band gaps of $(InAs)_6/(GaSb)_n$ and $(InAs)_8/(GaSb)_n$ superlattices.

The atomistic empirical pseudopotential method (AEPM), recently developed for the InAs/GaSb system, has been applied to calculate the fundamental band gap of InAs/GaSb superlattices with a fixed InAs layer thickness of n = 6 monolayers and n = 8 monolayers, respectively, and a variable GaSb layer thickness (m = 6, 9, 12. 18, 24 ML for n = 6, and m = 8, 12, 16, 24, 32, 40 ML for n = 8). The comparison with the results of FTIR absorption spectroscopy performed at AFRL has shown that the gaps predicted by AEPM are consistently smaller than the measured ones. The discrepancy is larger for the superlattices with a shorter GaSb layer. The calculated blue shift, 95 meV is larger than the experimental one, 70-75 meV. On the other hand, the SEPM approach predicts larger band gaps, in agreement with the experiment and the predicted blue shift is 49 meV. The values predicted by AEPM and SEPM are the best predictions obtained so far since other empirical pseudopotential calculations or the standard envelope function approximations are or unable to predict the blue shift of the band gap or strongly underestimate its value. To improve the agreement with the experimental data I tried to include in the theory a better description of the interfacial morphology. In fact the actually grown superlattices always show some atomic intermixing and disorder at the interfacial region. The interfacial segregation has been included by using a kinetic model of molecular beam epitaxy (MBE) growth whose parameters were obtained by fitting the X-STM measured Sb profiles in InAs. I simulated the composition profiles of all four atomic constituents, Ga, In, As, and Sb at the normal and inverted interfaces as a function of growth temperature and deposition rate. By taking into account the atomic segregation at the interfaces the agreement with the measured data is greatly

improved. Calculations performed using growth temperatures ranging from 380°C to 400°C and deposition rates from 0.5 ML/s to 1 ML/s give a very good agreement with the experiment. The predicted band-gap blueshifts for the segregated superlattices are 68 meV for the n = 8 case and 107 meV for the n = 6 case, in very good agreement with the experimental values 70-75 meV for the n = 8 case and 102-107 meV for the n = 6 case.

The calculated band gaps for the n = 8 case are shown here below in Fig. 1.

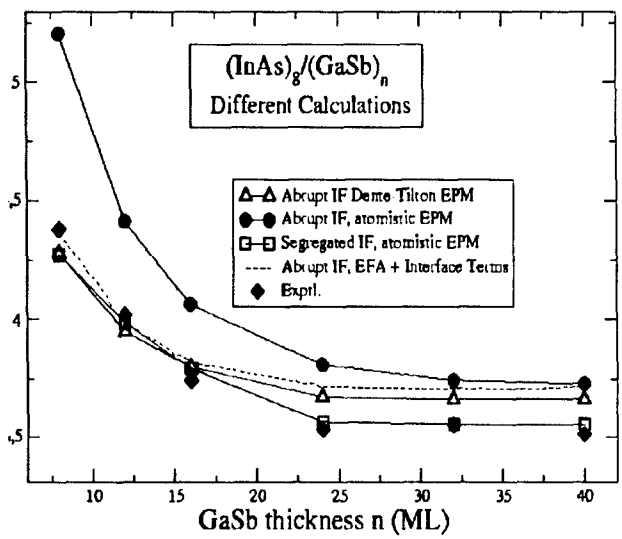

Fig. 1

2) Further tests of the AEPM.

I also studied in detail the performance of the AEPM method trying to predict the band gaps and band edges of ternary and quaternary systems (see below) and also analysing how well the method describes the interfaces between InAs and GaSb. In fact the AEPM extracts the atomic potential parameters by fitting the experimentally measured quantities, such as valence band offsets, band gaps, effective masses and deformation potentials, and few ab-initio calculated quantities, such as the single band deformation potentials, of ONLY the *unstrained* binary compounds InAs, GaSb, InSb and GaAs. Nothing guaranties that the interfaces between different binary compounds are well

described. The SEPM developed at AFRL assumes that the electronic charge at the hetero-interface redistributes so as to maintain the layer potentials as bulk-like as possible. The AEPM treats the abrupt interface using the full properties of the Ga-As and In-Sb epitaxially strained bonds. However the description of the effects of the charge transfer among the atomic planes at the interface is an open problem. I compared the charge redistribution and the total potential behaviour at the interfaces obtained with the AEPM with the analogous quantities obtained with an ab-initio method. The ab-initio methods have the advantage that they do not depend on empirical parameters but, unfortunately they are computationally heavy, so only relatively small systems can be described. Density functional theory in the local density approximation is known to provide a very good description of the ground state properties, among them the atomic structure and the electronic charge density redistribution. The calculations have shown that the charge rearrangement at the interface affects the charge/potential profile of only four atomic planes at the two sides of the interface. This strongly supports the approximation used in AEPM to consider only the first neighbour environment to construct the potential on the atom and also the approximation used in the SEPM that considers a quite abrupt potential change at the interfaces.

A direct comparison of the VBM and CBM wave functions obtained using the AEPM and the ab-initio approach is not possible due to the failure of the ab-initio method to produce a positive band gap (not a ground state property) at the Gamma point. Thus, I have calculated the Brillouin Zone integrated charge of the heavy hole band for a $(GaSb)_5/(InAs)_5$ superlattice with both methods. In this case the comparison can be done, since at the special points used for the charge integration the band gaps produced by the ab-initio method are positive. At the special points the gaps are large enough that the ab-initio method can separate the occupied and unoccupied states and correctly calculate the electronic charge. The comparison is given in Fig. 2. The AEPM method is able to reproduce very satisfactorily the much larger amplitude of the heavy-hole electronic charge at the In-Sb interface which is found also in the ab-initio calculation. This shows that the AEPM is able to reproduce correctly the charge transfer at the interfaces and the potential differences existing between the In-Sb and Ga-As interfaces.

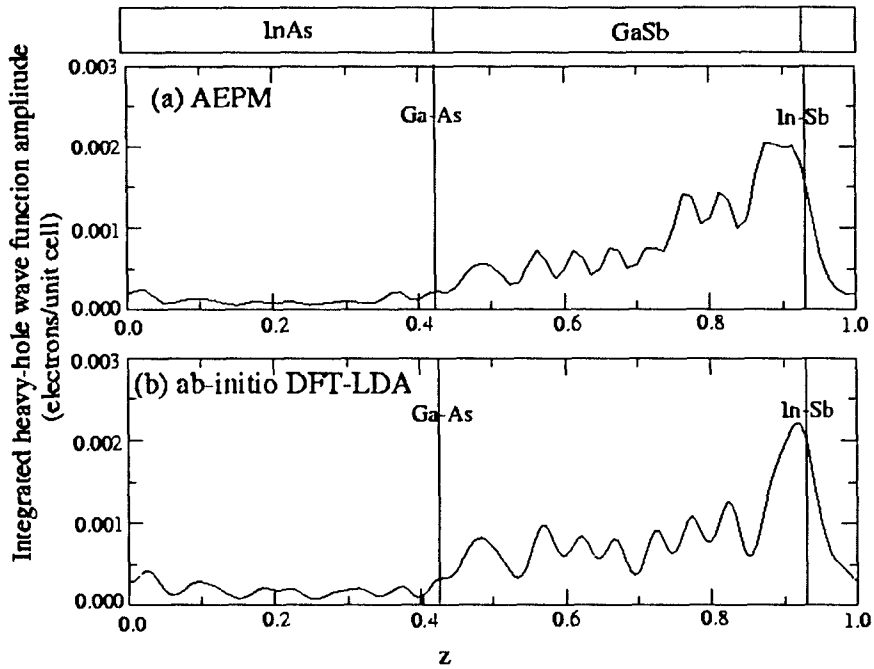

Fig. 2

During this year I had to adjust slightly the energy position of the valence band maximum of InSb to meet the advised value proposed recently in the literature (Vurgaftman and al., Journ. of Appl. Physics, **89**, 5815 (2001). Following that prescription, the entire band structure of InSb was shifted upward almost rigidly of 74 meV posing the InSb VBM 34 meV above the GaSb VBM. This has required a refit of the InSb pseudopotential parameters. The tests of the new potential has been performed and the comparison between the results obtained using the new and the old potentials for the InSb binary system, for the superlattices, and for the ternary alloys has been already reported in a previous performance report.

3) Valence and Conduction Band Edge Energies for Ternary Common Cation $GaAs_xSb_{1-x}$ and $InAs_xSb_{1-x}$ alloys.

This investigation was not part of the initially proposed research effort. However, during a visit at the CHTM in Albuquerque, New Mexico, USA with Ron Kaspi, Andrew Ongstad and Mike Tilton of AFRL, I was asked to perform calculations, using the developed AEPM, to predict the behaviour of the conduction and valence band edges in

ternary and quaternary systems constituted by GaSb and InAs. They were planning to design a new diode laser structure using ternary and quaternary compounds lattice-matched to a GaSb substrate and knowledge of band alignments between the components is a fundamental information for assessing a device performance. The idea under study at AFRL is to substitute the sequence InAs/$Ga_xIn_{1-x}Sb$/InAs with a sequence $InAs_{1-x}Sb_x$/$GaAs_ySb_{1-y}$/ $InAs_{1-x}Sb_x$ in order to have the main radiative emission line due to the recombination of the electron (in $InAs_{1-x}Sb_x$) with a light hole (in $GaAs_ySb_{1-y}$) instead of an heavy-hole as it happens in InAs/$Ga_xIn_{1-x}Sb$/InAs. In literature the conduction and valence band edges are obtained using methods based on a linear interpolation of the data

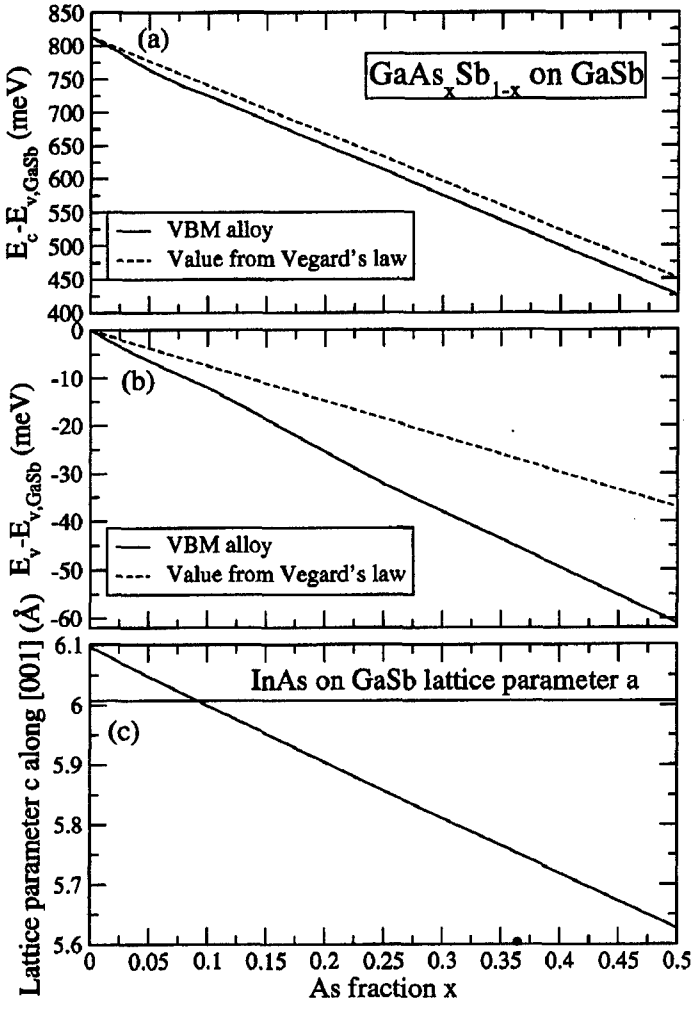

Fig. 3

relative to the binary and ternary systems, but it has been showed this to be a rather poor description.

I calculated using the atomistic EPM the trends of the conduction and valence bands in $GaAs_xSb_{1-x}$ in the composition range $0<x<0.5$ (Fig. 3) and $InSb_xAs_{1-x}$ in the composition range $0<x<0.5$ (Fig. 4).

I modelled perfectly random alloys using cubic cells with 512 atomic sites. The atomic sites were randomly occupied with Ga, In, As and Sb to obtain the desired alloy composition. Then, the elastic energies of the structures were minimized by allowing atomic displacements under the epitaxial constrain of lattice-matching to

GaSb, by using a Valence Force Field (VFF) approach. This procedure allowed me to obtain also the c-axis parameter along the [001] direction (which can be a measure of the deviation from the lattice-matched condition to the substrate) as a function of the alloy composition x. $GaAs_xSb_{1-x}$ is under biaxial tension on GaSb for $x > 0$, thus, a light hole is always the VBM as required. In $InSb_xAs_{1-x}$ (the electron well) there is a crossing between light-hole and heavy-hole at the VBM for $0.102 < x_c < 0.113$. I applied, then, the

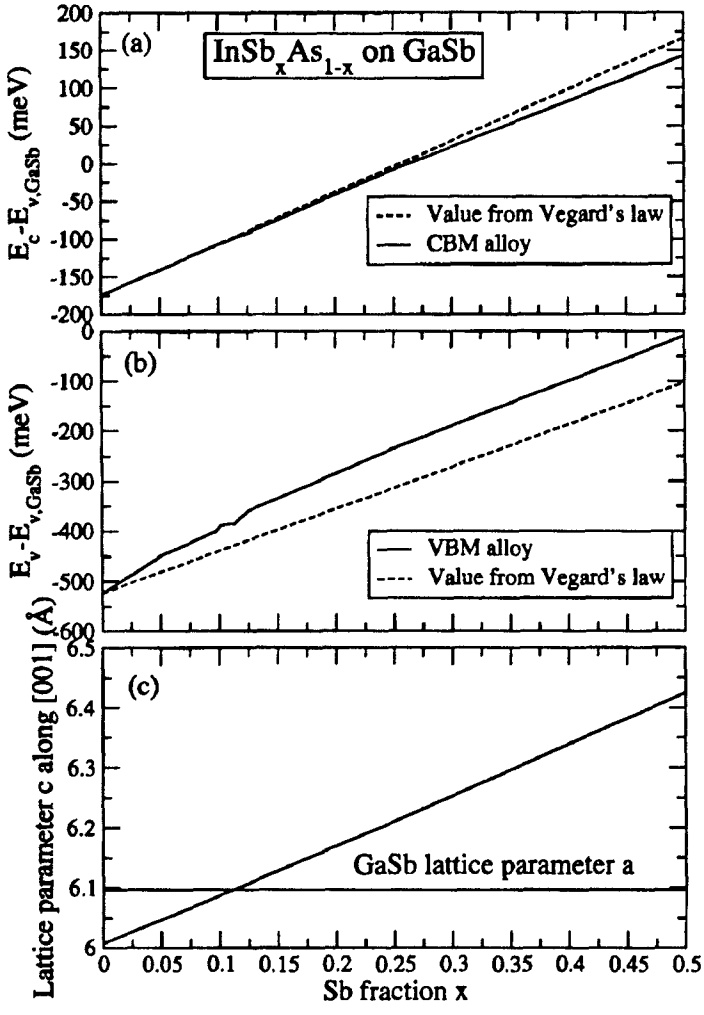

Fig. 4

AEPM to these models of the ternary random alloy. The calculations show that under the epitaxial constrain, the VBM of $GaAs_xSb_{1-x}$ (the hole well) has a slight *positive* (downward) bowing, while the VBM of $InSb_xAs_{1-x}$ has a much larger *negative* (upward) bowing. As a consequence, the sequence of strain compensated $GaAs_xSb_{1-x}$ and $InSb_yAs_{1-y}$ (the condition on the compositions x and y for strain compensation can be in a first approximation, obtained, from Fig. 3 c and fig. 4 c, considering the two compositions on the abscissas so that the two *c* values on the ordinates from the two figures, summed, give approximately the value of the lattice constant of GaSb), gives rise to a valence band offset between $InSb_yAs_{1-y}$ and $GaAs_xSb_{1-x}$ which diminishes progressively with increasing the compositions x and y. For the electron states the calculations show a *positive* (downward) bowing of the CBM both in $InSb_yAs_{1-y}$ and $GaAs_xSb_{1-x}$. The bowing

is larger for $GaAs_xSb_{1-x}$.Thus, even for the electron the confinement in $InSb_yAs_{1-y}$ diminishes by increasing the compositions x and y but the effect is smaller than for the hole states.

With the results of Fig. 3 and Fig. 4 is possible to design the conduction and valence band profiles of a device made up of GaSb, $InSb_yAs_{1-y}$, and $GaAs_xSb_{1-x}$ all grown on GaSb. Obviously, the kinetic effects due to MBE growth, the effects of short-range ordering and clustering (alloys are never perfectly random), and the charge redistribution due to interface potential effects change the fine details of these profiles and affect the performance. Finally, I calculated the bowing parameters of the epitaxially constrained ternary $InSb_xAs_{1-x}$ and $GaAs_xSb_{1-x}$ alloys. I found for $InSb_xAs_{1-x}$ a valence band bowing parameter b_v = -0.4/-0.5 eV, while the conduction band bowing is smaller and depends strongly on the composition x. It remains almost zero for $x < x_c$ then it increases until b_c = 0.125 at x = 0.75. Then, the band gap bowing parameter $b_g = b_c - b_v$ is about 0.4/0.5 eV and it is determined mainly by the bowing of the VBM. This value for b_g can be compared with the value b_g = 0.744 estimated at x = 0.75 for unstrained $InSb_xAs_{1-x}$ (that is not epitaxially constrained to a substrate). For $GaAs_xSb_{1-x}$ the valence band bowing $0.05 < b_v < 0.08$ is small, while the conduction band bowing parameter is larger, from 0.1 to 0.3.

4) Calculation of band edge energies and band gaps of the $Ga_{1-y}In_yAs_xSb_{1-x}$/GaSb and $Ga_{1-y}In_yAs_xSb_{1-x}$/InAs quaternary alloys as a function of composition (x,y).

Using atomistic empirical pseudopotentials (AEPM), I calculated the evolution of the conduction band minimum $E_c(x,y)$ and the valence band maximum $E_v(x,y)$ of the quaternary random $Ga_{1-y}In_yAs_xSb_{1-x}$ alloy grown on a GaSb and on a InAs substrate, as a function of composition x, y.

To address this problem I have modeled the $Ga_{1-y}In_yAs_xSb_{1-x}$ alloy by a large $4a_1 \times 4a_2 \times 4a_3$ supercell, where a_i are the conventional cubic cell lattice parameters, occupying its 512 lattice sites by the atoms Ga, In, As, and Sb according to specified compositions (x,

y). The atomic positions are then relaxed so as to minimize the total strain energy. Many, randomly created occupation patterns were then configurationally averaged. A atomic pseudopotential is assigned to each atom and the total pseudopotential is obtained by superposing all the individual pseudopotentials. The diagonalization of the corresponding Hamiltonian gives us the eigenvectors and eigenvalues, that is the band structure from which we extract $E_c(x,y)$ and $E_v(x,y)$.

The first step is then the determination of the alloy composition (x, y) at which the alloys are lattice matched to their substrate, that is $a(x, y) = a_{substrate}$. When this condition is verified the alloy grows with a cubic cell, with lattice parameter c along the growth [001] direction equal to the substrate lattice constant, $c(x, y) = a_{substrate}$. To study the dependence of the alloy cell lattice parameters a(x, y) from the composition (x,y) I used the atomistic valence force field (VFF) approach. The atomic positions and the cell lattice parameters are determined by minimising the total elastic energy by relaxing all the unconstrained internal and cell external degrees of freedoms. The predictions for the lattice parameters obtained via VFF have been compared with those of the commonly used continuum elasticity theory. I found small differences between the VFF predicted a(x, y) and c(x, y) lattice parameters and the lattice parameters obtained using the continuum elasticity. Moreover, in the case of the atomistic VFF modelling I found a slight dependence of the lattice parameters from the actual atomic configuration within the unit cell of the alloy.

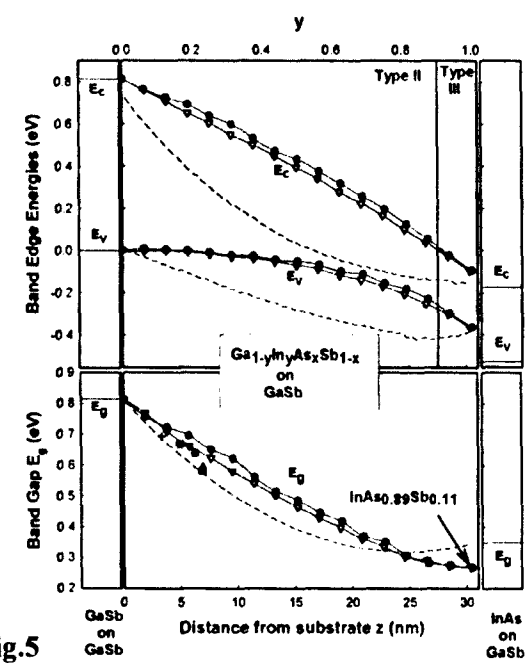

Fig.5

The VFF calculations show that at fixed In composition y, the configurations with the highest possible As fraction x, which can satisfy the lattice-matched condition c(x, y) = a_{GaSb}, have generally a lower elastic energy. The inspection of the bond composition shows that these structures have more In-As and Ga-Sb bonds (and correspondingly less In-Sb and Ga-As

bonds) than the averaged values determined by the alloy composition (x, y). This leads to a lower strain energy. I called $x = f_{VFF}(y)$ the lattice-matching condition obtained imposing $a(x, y) = a_{substrate}$ in the VFF calculation. A fit yields $x = 0.001 + 0.648\ y + 0.239\ y^2$ for the quaternary alloy grown on GaSb and $x = 0.0876 + 0.656\ y + 0.256\ y^2$ for the same quaternary grown on InAs. These lattice-matching conditions on the composition (x, y) show a larger bowing term (e. g. the coefficient of y^2) than the usually employed Vegard-like relations.

In the case of the GaSb substrate, I found that the dependence of $E_c(x,y)$ and $E_v(x,y)$ on y do not change considerably if we use the linear lattice matching condition $x = 0.89y$ instead of $x = f_{VFF}(y)$, where $x = 0.89$ is the As fraction in the ternary $InAs_xSb_{1-x}$ for which the ternary alloy is lattice-matched to GaSb (as calculated using the VFF method). The comparison is given in Fig. 5 where the band edges $E_v(x,y)$, $E_c(x,y)$, and the band gaps $E_g(x,y)$ corresponding to $x = f_{VFF}(y)$ are given by full dots while the values corresponding to $x = 0.89y$ are given by downward empty triangles.

The behavior of the band edges and band gaps are reported as a function of the distance Z from the GaSb substrate (bottom axis) when the alloy composition y is graded along the growth direction at the rate of 1% per monolayer. For comparison we show in figure also the conduction and valence-band edge position of $Ga_{1-y}In_yAs_xSb_{1-x}$/GaSb proposed by Turner and Choi. The atomistic (VFF+EPM) calculations predict a small but negative (upward) bowing of E_c and a pronounced positive (upward) bowing of E_v, in contrast with the trends given in literature. We have seen that the bowing of E_c is negative only when comparing with the *artificial* material obtained by the linear interpolation of the two end point GaSb and $InAs_{0.89}Sb_{0.11}$ materials (note that these "materials" would have a unphysically large number of GaSb and InAs bonds not obtainable in a real quaternary alloy). However, when properly compared

Fig. 6

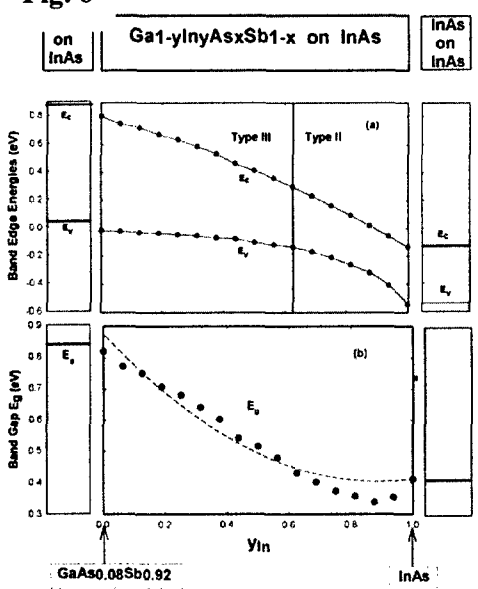

with the linearly-weighted band gaps of the four binary systems, $E_{ave}(x,y) = xyE_{InAs} + x(1-y)E_{GaAs} + (1-x)y\ E_{InSb} + (1-x)(1-y)E_{GaSb}$, we find that the alloy E_c is below $E_{ave}(x,y)$ suggesting that the physical bowing is indeed positive. From our calculation we find the transition from type II (staggered) to type III (broken-gap) at a relatively high content of In ($y = 0.92$ and $x = 0.81$). This is because of the small "bowing" of E_c. Our predicted transition from the staggered to the broken gap alignment at about $y = 0.92$ and $x = 0.81$ is in good agreement with recent experiments which found a type II staggered lineup for $y = 0.85$ and a broken gap lineup for $y = 0.95$. For $y = 0.92$ the authors observed both types of heterojunctions depending on temperature.

In Fig.6 we report the same predictions for $Ga_{1-y}In_yAs_xSb_{1-x}$/InAs. We see that the CBM of InAs dips below the VBM of the quaternary at $y = 0.62$. Very interestingly the quaternary reaches a well defined minimum gap at $y = 0.87$. The gap is 72 meV smaller than the InAs gap.

5) First-principles study of Sb-stabilized GaSb(001) surface reconstructions.

The starting point for understanding the mechanisms of the GaSb/InAs interface formation is a detailed knowledge of the stoichiometric and morphological properties of the surface on which adatoms are deposited.

The adatom kinetics on the surface is in fact determined by the potential energy (PES) landscape shaped by the initial surface reconstruction, that provides the template for islands nucleation. Since the behavior of GaSb(100) can be different from that of AlSb(001), as it happens in extreme Sb-rich conditions, we considered worthy to study the GaSb(001) surface phase diagrams. We energetically compared the reconstruction models schematically represented in Fig. 7, which were proposed in the literature on the basis of experimental observations of the GaSb(001) surface in typical MBE growth conditions, (GaSb growth is usually performed in Sb-rich conditions at temperatures around 500°C), with different structures having the same 4x3 geometry, but presenting a different surface stoichiometry.

We performed first-principle calculations based on the density functional theory in the local density approximation (DFT-LDA). The ionic species were described by

pseudopotentials, and the electronic wave functions were expanded in a plane-wave basis, with a kinetic energy cutoff of 18 Ry. The surface calculations were performed in the repeated supercell approach, using the equilibrium lattice parameters calculated for the bulk phase (6.005 Å).

In Fig. 8 the surface energies of the studied structures are plotted as a function of Ga chemical potential μ_{Ga} in an interval slightly larger than the allowed range. The ideal 1x1 unrelaxed surface with one complete Sb monolayer coverage is used as energy zero.

Different observations follow:

1) The c(6x2) reconstruction proposed by different experimental works, and violating the ECR (electron counting rule) is never favored: the formation energy of this surface is higher than that of the 4x3 phases in the range of variation of the Ga (and Sb) chemical potential, i.e. in a wide range of surface preparation conditions ranging from Ga-rich to Sb-rich. This result suggests that the ECR holds in general true for GaSb(001) as it happens for the other III-V semiconductor compounds, its violation is then related to the occurrence of exceptional Sb-rich conditions at GaSb(001).

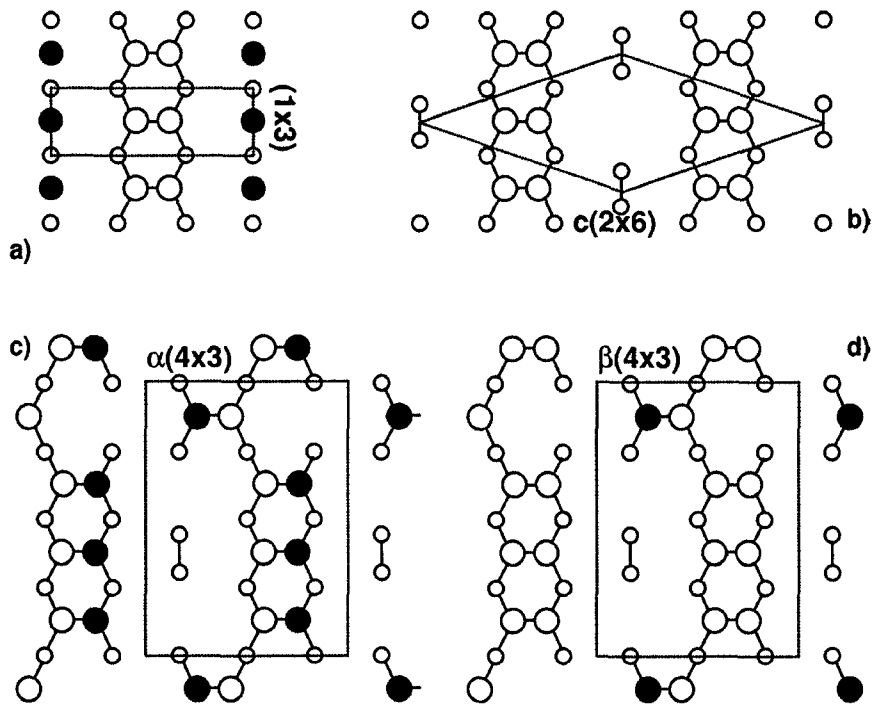

2) According to the calculated surface phase diagram of Fig. 8, three surface reconstructions can be observed at GaSb(001) surface: the 4x3 structure dominates when $\Delta\mu_{Ga}/H_f > 0.5$, i.e. when an excess of Ga is present at the surface. In slightly Sb-rich conditions, i. e. $\Delta\mu_{Ga}/H_f \in [-0.75, 05]$, which are the conditions under which GaSb growth usually takes place, the β(4x3) reconstruction is predicted to be the most favorable surface phase. In stoichiometric conditions, ($\Delta\mu_{Ga}/H_f \approx 0.5$) the β(4x3) reconstruction probably coexists with the d(4x3) and the t(4x3) structures, that present the same geometry but a different number of hetero-dimers, and have very close surface energies. If the amount of Sb at the surface is increased, ($\Delta\mu_{Ga}/H_f < -0.75$), our calculations suggest a surface phase transformation from the β(4x3) reconstruction to the z(4x3) reconstruction. The latter structure has never been reported in the literature. In order to predict whether the z(4x3) can indeed be experimentally observed, an energetic comparison with the (nx5)-like metallic reconstruction observed in extremely Sb-rich conditions is needed.

3) The formation of Ga dimers at the GaSb(001) surface is highly unfavored as demostrated by its energetic position in Fig. 8 corresponding to the ga-(3x4) structure.

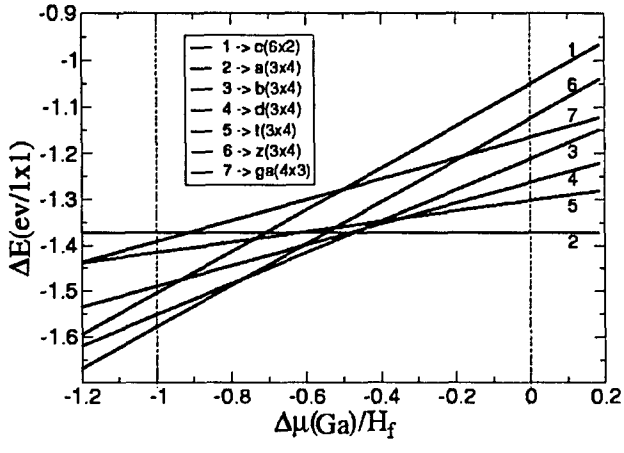

Fig. 8

6) Study of the As for Sb exchange mechanism on the Sb-stabilized reconstructed GaSb (001) surface.

In order to investigate the mechanisms of As/Sb exchange at the GaSb(001) surface we performed first-principles calculations based on the density functional theory in the local density approximation (DFT-LDA). We assumed that the arsenic impinging upon the surface forms As_2 molecules whereas antimony desorbs as Sb_2 molecules. We started by evaluating whether the substitution of two Sb atoms with two As atoms anywhere on the surface will cause an energy gain for the system. We simulated different As/Sb exchange configurations considering both the $\beta(4x3)$ and the $\alpha(4x3)$ surface reconstructions. Each final configuration of the exchange process is constructed by locating two As atoms (red spots in Fig. 9) in place of two Sb atoms belonging to the original reconstruction and then relaxing the system. The energy cost or gain of the As for Sb substitution was calculated by comparing the total energy of the system before, E_i, and after, E_f, the substitution. E_i (E_f) were calculated as a sum of the energy of one As_2 (Sb_2) molecule in the vacuum plus the energy of the GaSb(001) surface without (with) As substitution in place of Sb in the original surface reconstruction. In this way the initial and final systems have the same number of atoms and the energy difference $\Delta E = E_f - E_i$ can be accurately estimated. The values obtained for ΔE of each considered configuration are given in Fig. 9.

We see from our calculations that it is not energetically favourable a direct substitution of the Sb in-dimers or ad-dimers directly with the As_2 molecule, that is, a single As_2/Sb_2 exchange process is unlikely. Instead, we found that the anion exchange is favored with the Sb atoms belonging to the second Sb layer. In these cases the adsorbed As atoms form inward bonds with the third Ga layer and outward bonds with the dimers of the reconstruction. These results suggest that arsenic incorporation into the surface is more favourable when more Ga-As bonds can be formed, in agreement with the observation that the cohesive energy of GaAs is about 1.7 eV larger than the cohesive energy of GaSb. The most stable configuration is in fact shown in Fig. 9g, where the As atoms are coordinated as in GaAs bulk.

Our preliminary results show that (1) the trenches in the GaSb(001) surface reconstruction are probably highly reactive sites for the interaction between the As_2

molecule and the surface , and (2) before incorporation the As_2 molecule needs to break-up.

We are currently investigating these issues.

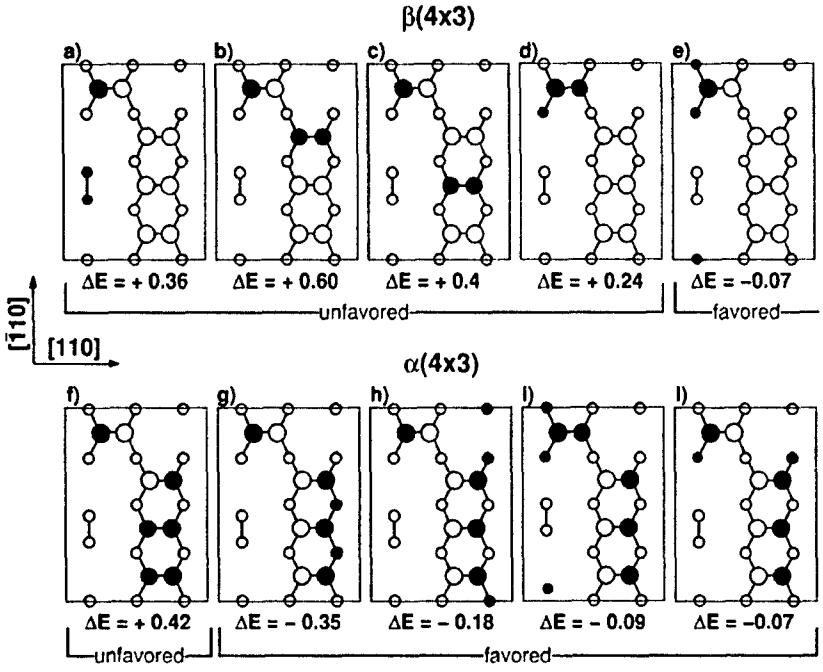

Fig. 9

Published Papers

1) **Rita Magri** and Alex Zunger,
"*Theory of Optical properties of 6.1 A III-V Superlattices: the Role of Interfaces*",
Journal of Vacuum Sci. & Technol. B **21**, 1896 (2003) (WOS support acknowledged)

2) **R. Magri** and A. Zunger,
"*Theory of Optical Properties of segregated InAs/GaSb Superlattices*",

IEE Optoelectronics **150**, 409 (2003). (WOS support acknowledge)

3) **Rita Magri** and Alex Zunger,
"*Predicting Interband Transition Energies for InAs/GaSb Superlattices using the Empirical Pseudopotential Method*"
Phys. Rev B **68**, 155329 (2003)
(acknowledged EOARD support)

Papers accepted for publication (in print)

4) M. C. Righi, **Rita Magri**, and C. M. Bertoni,
"*First-principles study of Sb-stabilized GaSb(001) surface reconstructions*"
Phys. Rev. B, in print (EOARD support acknowledged)

5) M. C. Righi, **Rita Magri**, and C. M. Bertoni,
"*First-principles study of GaSb(001) surface reconstructions*"
ICPS2004 Proceedings (2004) in print

Submitted papers

6) Rita Magri, Alex Zunger, and H. Kroemer,
"*Evolution of the band gap and band edge energies of the lattice-matched GaInAsSb/GaSb and GaInAsSb/InAs alloys as a function of composition*"
submitted to Journal of Applied Physics (EOARD support acknowledged)

Acknowledgement of Sponsorship: Effort sponsored by the Air Force Office of Scientific Research, Air Force Material Command, USAF, under grant number FA8655-03-1-3017. The U.S. Government is authorized to reproduce and distribute reprints for Government purpose notwithstanding any copyright notation thereon.

Conferences

1) **Rita Magri**, and A. Zunger,

"Optical Properties of segregated InAs/GaSb Superlattices"
MIOMD-V Annapolis, Maryland, USA (September 9, 2002).

2) R. Magri and A. Zunger,
"*Theory of optical properties of 6.1 Å III-V superlattices: the role of the interfaces*"
PCSI-30: 30th Conference on the Physics and Chemistry of Semiconductor Interfaces, January 19-23, 2003, Salt Lake City, Utah, USA.(**invited talk**).

3) R. Magri and A. Zunger,
"Predicting energy gaps in InGaAsSb Superlattice and Alloy Systems usng the Empirical Pseudopotential Method", 11th International Conference on Narrow Gap Semiconductors, June 16-20, 2003, Buffalo, New York, USA, (**invited talk**).

4) R. Magri, A. Zunger, and H. Kroemer, "*Evolution of the band gaps and band edges of ternary $GaAs_xSb_{1-x}$, $InAs_xSb_{1-x}$, and quaternary $Ga_{1-y}In_yAs_xSb_{1-x}$/GaSb and $Ga_{1-y}In_yAs_xSb_{1-x}$/InAs alloys as a function of composition*", 6th International Conference Mid-Infrared Optoelectronics Materials and Devices (MIOMD-6), June 28-July 02, 2004, St. Petersburg, Russia (oral).

5) R. Magri,
"*Band Gaps and Band Edges of InGaAsSb Superlattice and Alloy Systems for Infrared Device Applications*", IVC-16 (16th International vacuum Congress)-ICSS-12 (12th International Conference on Solid Surfaces) –NANO-8 (8-th International Conference on Nanometer-Scale Science and Technology), June 28-July 02, 2004, Venice, Italy (Oral).

6) R. Magri, A. Zunger, and H. Kroemer, ICPS-27, 27th International Conference on the Physics of Semiconductors, July 26-30, 2004, Flagstaff, Arisona, USA

Seminar and visit at CHTM, Albuquerque, New Mexico, USA.

Jan. 23 – 28, 2003. I visited the CHTM where I had a metting with R. Kaspi, M. Titlon, A. Ongstad of AFRL. I gave also a IEEE/LEOS Lecture at CHTM on "*Theory of Optical Properties of 6.1 Å III-V Materials*".

I certify that there were no subject inventions to declare during the performance of this grant

REPORT DOCUMENTATION PAGE

Form Approved OMB No. 0704-0188

1. REPORT DATE *(DD-MM-YYYY)*	2. REPORT TYPE	3. DATES COVERED *(From – To)*
13-01-2005	Final Report	12 November 2002 - 17-Mar-05

4. TITLE AND SUBTITLE

Empirical Pseudopotential Modeling of Antimonide-Based III-V Structures

5a. CONTRACT NUMBER
FA8655-03-1-3017

5b. GRANT NUMBER

5c. PROGRAM ELEMENT NUMBER

6. AUTHOR(S)

Dr. Rita Magri

5d. PROJECT NUMBER

5d. TASK NUMBER

5e. WORK UNIT NUMBER

7. PERFORMING ORGANIZATION NAME(S) AND ADDRESS(ES)
National Institute for the Physics of Matter (INFM)
University of Modena e Reggio Emilia
Via G. Campi 213/A
Modena 41100
Italy

8. PERFORMING ORGANIZATION REPORT NUMBER
N/A

9. SPONSORING/MONITORING AGENCY NAME(S) AND ADDRESS(ES)

EOARD
PSC 802 BOX 14
FPO 09499-0014

10. SPONSOR/MONITOR'S ACRONYM(S)

11. SPONSOR/MONITOR'S REPORT NUMBER(S)
SPC 03-4017

12. DISTRIBUTION/AVAILABILITY STATEMENT

Approved for public release; distribution is unlimited.

13. SUPPLEMENTARY NOTES

14. ABSTRACT

This report results from a contract tasking National Institute for the Physics of Matter (INFM) as follows: The contractor will make a detailed comparison of the conventional Empirical Pseudopotential Model (EPM) with the Superlattice Empirical Pseudopotential Model (SEPM) developed at AFRL, by comparing the predictions of the two methods for the transition energies in a number of well characterized and microscopically controlled InAs/GaSb Type-II superlattice samples. The comparison between the two different implementations of the empirical pseudopotential method and with the experiment will lead to a better understanding of the role of the transition energies and dipole matrix elements of the interface bonds in the no-common-atom InAs/GaSb superlattices and how they can be adequately described by the theory. This is a necessary step in the direction of making the EPM a reliable tool for analyzing and predicting behavior and performances of the devices based on antimonide III-V semiconductors.

15. SUBJECT TERMS
EOARD, Mid-IR lasers, Nanotechnology, Semiconductor materials

16. SECURITY CLASSIFICATION OF:			17. LIMITATION OF ABSTRACT	18, NUMBER OF PAGES	19a. NAME OF RESPONSIBLE PERSON
a. REPORT	b. ABSTRACT	c. THIS PAGE			MATTHEW MORGAN, Lt Col, USAF
UNCLAS	UNCLAS	UNCLAS	UL	16	19b. TELEPHONE NUMBER *(Include area code)* +44 (0)20 7514 4505